Studies on the relationship between pulsed UV light irradiation and the simultaneous occurrence of molecular and cellular damage in clinically-relevant *Candida albicans*

Hugh Farrell [a], Jennifer Hayes [a], John Laffey [b], Neil Rowan [a],*

[a] Department of Nursing and Health Science, Athlone Institute of Technology, Ireland
[b] Department of Anaesthesia and Critical Care Medicine, National University of Ireland Galway, Ireland

ABSTRACT

This constitutes the first study to report on the relationship between pulsed UV light (PL) irradiation and the simultaneous occurrence of molecular and cellular damage in clinical strains of *Candida albicans*. Microbial protein leakage and propidium iodide (PI) uptake assays demonstrated significant increases in cell membrane permeability in PL-treated yeast that depended on the amount of UV pulses applied. This finding correlated well with the measurement of increased levels of lipid hydroperoxidation in the cell membrane of PL-treated yeast. PL-treated yeast cells also displayed a specific pattern of intracellular reactive oxygen species (ROS) generation, where ROS were initially localised in the mitochondria after low levels of pulsing (UV dose $0.82 \mu J/cm^2$) before more wide-spread cytosolic ROS production occurred with enhanced pulsing. Intracellular ROS levels were measured using the specific mitochondrial peroxide stain dihydrorhodamine 123 and the cytosolic oxidation stain dichlorofluorescin diacetate. Use of the dihydroethidium stain also revealed increased levels of intracellular superoxide as a consequence of augmented pulsing. The ROS bursts observed during the initial phases of PL treatment was consistent with the occurrence of apoptotic cells as confirmed by detection of specific apoptotic markers, abnormal chromatin condensation and externalisation of cell membrane lipid phosphatidylserine. Increased amount of PL-irradiation (ca. UV does $1.24–1.65 \mu J/cm^2$) also resulted in the occurrence of late apoptotic and necrotic yeast phenotypes, which coincided with the transition from mitochondrial to cytosolic localisation of ROS and with irreversible cell membrane leakage. Use of the comet assay also revealed significant nuclear damage in similarly treated PL samples. Although some level of cellular repair was observed in all test strains during sub-lethal exposure to PL-treatments (≤ 20 pulses or UV dose $0.55 \mu J/cm^2$), this was absent in similar samples exposed to increased amounts of pulsing. This study showed that PL-irradiation inactivates *C. albicans* test strains through a multi-targeted process with no evidence of microbial ability to support cell growth after ≤ 20 pulses. Implications of our findings in terms of application of PL for contact-surface disinfection are discussed.

© 2010 Published by Elsevier B.V.

1. Introduction

The incidence of nosocomial yeast infections has increased markedly in recent time and has become a major cause of morbidity and mortality in vulnerable groups including neonates, cancer patients and the elderly (Fanello et al., 2001). More than 90% of persons infected with HIV who are not receiving highly active antiretroviral therapy eventually develop oropharyngeal candidiasis (de Repentigny et al., 2004). Prevention of infection is a superior approach compared to the cost and consequences of treatment of infection, with strong emphasis placed on hand hygiene compliance and proper cleaning regimens that include use of effective surface decontamination techniques (Solberg, 2000).

Pulsed UV light (PL) technology has received considerable attention as a promising next-generation approach for decontaminating food, packaging, water and air (Gómez-López et al., 2007; Elmnasser et al., 2007; Garvey et al., 2010a,b). This approach kills microorganisms by using ultrashort duration pulses of an intense broadband emission spectrum that is rich in UV-C germicidal light (200–280 nm band). PL is produced using techniques that multiplies power manifold by storing electricity in a capacitor over relatively long times (fractions of a second) and releasing it in a short time (millionths or thousandths of a second) using sophisticated pulse compression techniques (Rowan et al., 1999; Gómez-López et al., 2007). The emitted flash has a high peak power and usually consists of wavelengths from 200 to 1100 nm broad spectrum light enriched with shorter germicidal wavelengths (Wang et al., 2005; Gómez-López et al., 2007). A strong advantage of using pulsed xenon lamps over continuous low to medium pressure conventional UV lamps is that the former has a characteristic high peak-power dissipation, which allows for more rapid microbial inactivation. A continuous 10 W lamp needs

* Corresponding author. Department of Nursing and Health Science, Athlone Institute of Technology, Dublin Road, Athlone, Co. Westmeath, Ireland. Tel.: +353 906473081; fax: +353 906486135.
E-mail address: nrowan@ait.ie (N. Rowan).

to be operated for 10 s to achieve the same decontamination efficacy (supplying same energy) as a pulsed lamp of typically 1 MW operated for just 100 μs. Despite significant interest in the development of PL as an alternative or complementary means of disinfection, most published studies to date have only used conventional aerobic plate counts to report on gross microbial viability post UV irradiation. Moreover, with the exception of a limited study undertaken by Takeshita et al. (2003) no other published research has reported on the inter-related cellular responses involved in microbial response to pulsed light treatments. This dearth in microbial physiology data is critical as it may unlock key information for the subsequent development and optimization of this novel decontamination technology for surface, water and air applications.

This constitutes the first study to report on the relationship between the occurrence and augmentation of nuclear and cellular damage and apoptosis in clinically-relevant *Candida albicans* cells as a consequence of increased amounts of pulsed UV light treatments.

2. Materials and methods

2.1. Preparation and pulsing of C. albicans stains with UV rich light

A bench-top pulsed power source (PUV-1, Samtech Ltd., Glasgow) was used to power a low-pressure (60 kPa) xenon-filled flashlamp (Heraeus Noblelight XAP type NL4006 series constructed from a clear UV transparent quartz tube), that produced a high-intensity diverging beam of polychromatic pulsed light, was used in this study following the method of Farrell et al. (2009) with modifications. The pulsed light has a broadband emission spectrum extending from the UV to the infrared region with a rich UV content and its intensity also depends on the level of the voltage applied. The manufacturer stated that the discharge tube represents a line-source of limited length and consequently the light formed an elliptical, equi-intensity profile over the sample plane eliminating shading effects. This resulted in a ~30% variation in luminous intensity between the centre and the edge of the sample. The light source has an automatic frequency-control function that allows it to operate at one pulse per second that was used throughout this study. Light exposure was homogeneous as the xenon lamp measuring 9 cm × 0.75 cm was longer than the 8.5 cm diameter polystyrene Petri dishes used in the tests, which were placed directly below the lamp. For standard treatments, the light source was mounted at 8 cm above the treatment area that was designed specifically to accommodate a standard Petri dish containing 10 ml of sample and was set as the minimum or lower threshold distance by the fabricant. This was to ensure that full coverage of the Petri dish occurred and to eliminate possible shading effects.

Test microorganisms used in these experiments, their origin and clinical relevance are summarized in Table 1. All test strains were maintained in Microbank storage vials (Cruinn Diagnostic, Ireland) at −70 °C. Identification of three randomly selected isolates of each yeast strain was confirmed before and after experimental studies by use of the germ-tube assay with occasionally use of the VITEK yeast biochemical card and API-32 C systems (bioMérieux, France) as per methods described by Hsu et al. (2003). Strains were stored at 4 °C on agar slopes of Malt Extract agar (MEA; Oxoid, Basingstoke, UK) and

checked monthly for purity and renewed. To prepare the test samples, yeast test strains were streaked to purity from porous beads taken from Microbank vials, and an isolated colony was then transferred to 50 ml Malt Extract broth (MEB adjusted to pH 5.6 ± 0.2 °C; Oxoid, Basingstoke, UK) and cultivated with shaking at 125 oscillations per minute for 14 h at 35 °C until each test organism (listed in Table 1) reached late exponential phase as reported previously by Farrell et al. (2009). The optical densities of test samples were then spectrophotometrically adjusted at 640 nm to 0.2 units (ca. 10^8 CFU/ml) [Model UV-120-02 instrument, Shimadzu Corp., Kyoto, Japan] using 0.1 M phosphate buffered saline (PBS) [pH 7.2] (confirmed via aerobic plate count). Standard UV treatments involved re-suspending OD_{640nm}-adjusted yeast samples in sterile 10 ml of 0.1 M PBS, which was aseptically transferred to 8.5 cm Petri dishes and subjected to UV light treatments. The number of pulses of light used ranged from 0 (untreated control) to 150 pulses using a lamp discharge energy of 7.2 J at a distance of 8 cm from the light source that was shown previously to inactivate test yeast populations by ca. 7 log CFU/ml over this treatment regime (Farrell et al., 2009). Measurement of corresponding fluence rate (or 'irradiance) (Joule/cm^2) at each applied pulse was determined using chemical actinometry as described by Rahn et al. (2003), as the non-continuous emitted spectrum did not facilitate use of a calibrated radiometer. Dose is sometimes used as a synonym of fluence. The lethality of this PL process was confirmed by enumerating survivors post-treatments on triplicate Sabouraud dextrose agar (SDA; Oxoid) and MEA plates (both adjusted to pH 5.6 ± 0.2 °C) using the spread plate technique (expressed in terms of $\log_{10}$ colony forming units or CFU ml^{-1}). After 48 h at 35 °C, typically with the highest dilution, identify was confirmed as described above. All experiments were carried out in triplicate using the same culture to avoid sample variability. Heating of the yeast suspensions was measured using a thermocouple and by thermal imaging (IRI 4010, InfraRed Integrated Systems Ltd, Northampton, England) using modifications of Nugent and Higginbotham (2007). There was no discernable increase in saline temperature during UV treatments.

2.2. Determining yeast cell membrane integrity post UV treatments using microbial protein leakage and propidium iodide dye uptake assays

Damage or disruption to the cell membrane of test yeast was determined by measuring loss of intracellular proteins released into sample supernatant post-UV-irradiation at each PL-treatment endpoint. Treated and untreated yeast cell suspensions were kept on ice to prevent protease activity, centrifuged at 10,000 rpm for 10 min at 10 °C, and the supernatant was collected thereafter. The concentrations of eluted yeast protein in the supernatants were determined spectrophotometrically using the BSA Protein assay kit (Pierce Chemical) using 150 μl sample aliquots. The absorbances of PL-treated samples, untreated controls and BSA standards (range 0–200 μg BSA/ml) were measured at 560 nm after 2 h incubation at 37 °C on a micro-titre plate reader (Wallac 1420 VICTOR^2™ Turku, Finland). The standard curve of increasing concentration of BSA standard (μg/ml) against corresponding absorbance (560 nm) (data not shown) was used to determine the protein concentration of all PL-treated samples and untreated controls.

Non-permeable propidium iodide (PI) dye was also used to investigate disruption of cell membranes in similarly treated samples. When used in combination with the membrane-permeable fluorescent 4′,6-diamidino-2-phenylindole (DAPI) stain that binds strongly to DNA, it is possible to determine the proportion of cells with permeabilized cell membranes post UV treatments. 500 μl aliquots of treated cell suspensions (approx 10^7 cell ml^{-1}) were transferred to sterile Eppendorf tubes. Propidium iodide (Sigma) was added to a concentration of 100 μg/ml and the tubes were then incubated in the dark for 30 min at 4 °C. The cell suspension was subsequently counter

stained with 1 µg/ml DAPI. The cell suspension was then washed twice and resuspended in fresh PBS. A 20 µl aliquot of cell suspension from treated and control samples was transferred to a clean microscope slide, then mounted with glycerol gelatin (Sigma) and subsequently examined by fluorescence microscopy (Leitz Diaplan, Germany). All samples were examined in triplicate.

2.3. Measurement of reactive oxygen species (ROS) produced in UV irradiated test yeast

Overproduction of ROS in yeast cells as a consequence of UV irradiation was determined by using a number of oxidative-stress-sensitive probes namely: dihydrorhodamine 123 (DHR 123), 2′,7′-dichlorodihydrofluorescein diacetate (DCFH-DA) and dihydroethidium (DHE) (all probes were purchased from Sigma). Following UV treatments, 500 µl aliquots samples were separately transferred to a sterile Eppendorf tube. Thereafter, DHR-123 was added to a concentration of 5 µg/ml, and the tube was then incubated for 2 h at 30 °C in the dark. The oxidation of nonfluoresecnt DHR 123 to the fluorescent rhodamine 123 is catalysed by the enzyme peroxidase that accumulates in mitochondrial membranes (Nomura et al., 1999; Qin et al., 2008). The oxidation of DHR 123 was measured fluorimetrically using excitation and emission wavelengths of 505 and 535 nm. DCFH-DA was added to similarly treated samples at a final concentration of 10 µM from a 1 mM stock solution in ethanol, and then incubated at 30 °C for 1 h in the dark. The acetyl groups in DCFH-DA are removed by membrane esterases to form 2′,7′-dichlorodihydrofluorescein (DCFH) when this probe is taken up by viable cells. DCFH is not fluorescent but is highly sensitive to ROS (such as RO_2, RO, OH, $HOCl$, and $ONOO^-$) and is oxidised to the highly fluorescent compound 2′,7′-dichlorofluorescein via reactions described previously by Ischiropoulos et al. (1999). Exposure of samples to light was minimised, and fluorescence was measured spectro-fluorometrically (Wallac 1420 VICTOR^2™ Turku, Finland). Dihydroethidium (DHE) was added to a concentration of 5 µg/ml, and then incubated for 10 min at room temperature (DHE is oxidised to the fluorescent ethidium (ET) and is relatively specific for O_2^-, with minimal oxidation induced by H_2O_2, $ONOO^-$, or $HOCl$ as observed previously by Tarpey and Fridovich (2001). The cell suspension was subsequently counter-stained with 1 µg/ml DAPI. The cell suspension was then washed twice and resuspended in fresh PBS. 20 µl aliquot test samples and untreated controls were transferred to a clean microscope slide, mounted with glycerol gelatin (Sigma) and examined by fluorescence microscopy (Leitz Diaplan, Germany).

2.4. Measurement of lipid hydroperoxides production in UV irradiated yeast

A PeroxiDetect™ kit was used to determine the levels of lipid hydroperoxides in yeast cell lysate, which is based on a modified ferrous oxidation/xylenol orange assay of Jiang et al. (1991). Lipid peroxides oxidize Fe^{2+} to Fe^{3+} ions at acidic pH that form a colour adduct with xylenol orange (XO, 3,3′-bis[N,N–bis (carboxymethyl) aminomethyl]-o-cresolsulfonephthalein, sodium salt), which is observed at 560 nm. The cell lysate was prepared as described by Jiang et al. (1991). Test yeast cell suspensions were UV-treated as outlined above. Samples (5 ml) were harvested and washed twice with distilled water (15,000 rpm for 5 min at 4 °C). Cell pellets were subsequently transferred to 13×100-mm glass culture tubes and resuspended in 300 µl of methanol/0.01% butylated hydrotoluene (BHT). Approximately 1 g of glass beads was added, and the cells were lysed by vortexing (4 cycles of 30 s vortex, 30 s on ice), and the upper methanol layer was transferred to a microcentrifuge tube. The glass beads were then washed once with 1 ml of methanol/0.01% BHT, the methanol layers were pooled, and following centrifugation (100,000 rpm for 10 min at 4 °C) the supernatants were assayed for oxidation products. A *tert*-butyl hydroperoxide (*tert*-BuOOH) standard curve was prepared in 90% methanol [data not shown]. Working reagent was prepared by mixing 100 µL of ferrous ammonium sulphate Reagent (2.5 mM ammonium ferrous (II) sulphate/0.25 M sulphuric acid), and 10 ml of organic peroxide colour reagent (4 mM BHT/125 µM xylenol orange in 90% methanol). Samples of yeast cell lysate (100 µL) were added to 1 ml of working reagent. Samples were incubated at room temperature for 30 min, and the absorbance at 560 nm was measured.

2.5. Measurement of apoptosis in UV irradiated yeast

The following studies were undertaken to investigate the occurrence of cellular apoptosis and necrosis in PL-treated test yeast. Translocation of lipid phosphatidylserine (PS) from the inner leaflet to the extracellular side of the plasma membrane is an early stage event in apoptosis and was detected by using the Annexin V-FITC Apoptosis Detection kit (Sigma) as described by Madeo et al. (1999) with modifications. Annexin V stain has a strong binding affinity for PS. After PL-treatments, cells were harvested and washed with sorbitol buffer (1·2 M sorbitol, 0·5 mM $MgCl_2$, 35 mM K_2HPO_4, pH 6·8). Cell walls were digested with 60 U lyticase ml/L in sorbitol buffer (Sigma) for about 60 min at 28 °C, where digestion with this enzyme was carefully monitored by phase-contrast microscopy in order to prevent damage to the unfixed protoplasts. Cells were then washed twice with binding buffer (10 mM HEPES/NaOH, pH 7·4, 140 mM NaCl, 2·5 mM $CaCl_2$; CLONTECH Laboratories) containing 1·2 M sorbitol. To 38 µl cell suspensions in binding/sorbitol buffer were added 2 µl Annexin V (20 µg/ml) and 2 µl of a prodidium iodide (PI) working solution and incubated for 20 min at room temperature. The cells were then washed three times and resuspended in binding/sorbitol buffer. Finally the 10 µl of cell suspensions were transferred to clean microscope slides and mounted with the glycerol gelatine. Slides were observed using a Hamamatsu Colour chilled 3cco camera, attached to fluorescence microscope (Leitz Diaplan, Germany) at $40\times$ and $100\times$ magnification. For quantitative assessment of Annexin V$^-$ PI staining, at least 200 yeast cells were counted per sample and trials were repeated in duplicate. This combined Annexin V/PI staining approach enables distinction of early apoptotic (designated as Annexin V$^+$/PI$^-$), late apoptotic (designated as Annexin V$^+$/PI$^+$) and necrotic (designated as Annexin V$^-$/PI$^+$) cells. Chromatin morphology was also examined using DAPI stain as apoptotic cells demonstrate abnormal chromatin condensation with fragments forming a semicircle as described previously by Herker et al. (2004a,b). The **Q3** chromatin of untreated control samples appear as a single round spot in the middle of the cell. The standard protocol for DAPI nuclei staining was used as described by Klassen and Meinhardt (2004). Treated and **Q4** untreated cells were collected by centrifugation at 10,000 rpm for 10 min, then resuspended in 70% (v/v) ethanol and incubated for 1 h for fixation and permeabilisation. Following washing and rehydration in PBS, cells were resuspended in PBS containing 1 µg ml/L DAPI and visualized under a fluorescence microscope (Leitz Diaplan, Germany).

2.6. Detection of genotoxic damage in PL-irradiated test yeast using the comet assay

A modified alkaline comet assay procedure of Miloshev et al. (2002) was used in the present study for detecting and analyzing the ability of PL irradiation to cause DNA damage that includes strand breaks. *C. albicans* test strains were inoculated into separate 100 mL malt extract broth (Fluka) and incubated in a shaking incubator (New Brunswick Scientific Innova 4000) at 35 °C and 125 oscillations per minute for 18–24 h. The broth was centrifuged at 1400 rpm (Mistral MSE 1000 benchtop centrifuge), the supernatant discarded and the pelleted yeast cells resuspended in sterile PBS to a population density of ~10^7 cells/mL (confirmed via plate counts). 10 mL aliquots were

distributed into sterile Petri dishes and each dish was individually exposed to UV irradiation regimes as outlined earlier. Three 10 mL aliquots were incubated in 0.1 mM, 0.5 mM and 1 mM H_2O_2 respectively. These samples served as positive controls. A solution (referred to hereafter as SCE) containing 1.0 M sorbitol, 0.1 M sodium citrate and 60 mM EDTA was prepared. The irradiated yeast suspensions were collected in centrifuge tubes and centrifuged at 1000 rpm for 10 min. The pellets were washed twice in 10 mL 40 mM EDTA/ 90 mM 2-mercaptoethanol (known hereafter as 2-ME), discarding the supernatant. 2 mL SCE, 16 µL 2-ME and 0.2 mg lyticase were added to each centrifuge tube to resuspend the washed pellets. The tubes were incubated at 37 °C for 2 h in order to produce spheroplasts. A lysis buffer was prepared, consisting of 50 mM TrisHCl; 25 mM EDTA; 0.5 M NaCl; 3 mM $MgCl_2$; 3 mM 2-mercaptoethanol; 0.1% (v/v) Triton-X-100; and 10% (v/v) SDS. After the 2 h incubation period, the tubes were again centrifuged at 650 rpm for 10 min and the supernatant discarded. Each pellet was resuspended in 700 µL lysis buffer and incubated at 68 °C for 15 min, vortexing intermittently during this time. 200 µL of each sample was mixed with 400 µL 0.7% (w/v) low-melting point (LMP) agarose (previously boiled and then cooled to ~40 °C prior to mixing) and then spread thinly and evenly on to glass slide and immediately covered with a Gelbond®, Electrophoresis Film, (Sigma-Aldrich, Ireland) strip and stored at 4 °C for 10 min until the gel had set. Alkaline electrophoresis was preceded by a 20 min unwinding step in electrophoresis buffer pH13. Electrophoresis was performed in at 25 V and 300 mA for 12 min in a 2 L capacity 35 cm tank connected to Power Pac 300 (Bio-Rad), with gelbond strips placed horizontally side by side avoiding gaps. Yeast cells were neutralized by rinsing 3 times with Tris–Cl buffer pH 7.4 before fixation in 100% methanol for a minimum of 3 h at 4 °C. Prior to analysis, DNA was stained by placing gelbond strips in freshly prepared SYBR® Gold nucleic acid stain (Invitrogen GmbH, Germany) for 40 min at room temperature. Finally, the gels were cover-slipped and viewed at 400× magnification using a fluorescent microscope (Leitz Diaplan) equipped with an excitation filter of 475–490 nm.

2.7. Detection of photo-reactivation in UV-irradiated yeast

This experiment was designed to investigate the degree of photo-reactivation in PL-treated test yeast following the method of Farrell et al. (2010). Briefly, plates were prepared by spread plating 50 µl of cell suspension on relevant solid media in triplicate for each exposure. The plates were exposed to increasing doses UV irradiation as per regimes described earlier. The first three plates were immediately wrapped in aluminium foil post treatment; the remaining three plates were exposed to direct sunlight for 4 h post-treatment. The plates were incubated for 48 h at 37 °C. To determine the number of surviving cells, colonies were counted and expressed as $\log_{10}$ colony forming units (CFU)/cm^2. The experiment was conducted in triplicate and variance determined.

2.8. Statistical analysis

Student's t-tests and ANOVA one-way model (MINITAB software release 13; Mintab Inc., State College, PA) were used to compare the effects of the relationship of independent variables on light treatments.

3. Results and discussion

3.1. Determination of cell membrane integrity and functionality post pulsed light treatments

The integrity of yeast cell membrane in response to separate PL was determined using protein leakage and the combined PI/DAPI cell staining assays. Propidium iodide (PI) has been previously used as an indicator of microbial cell membrane functionality (Helmerhorst et al., 1999) as PI is able to enter permeabilised cells. Once in the microbial cytoplasm PI binds to nucleic acids yielding fluorescence in the red wavelength region (Virto et al., 2005). The relationships between cell vitality (determined by PI/DAPI staining), cell viability (determined by total aerobic plate counts) and concentration of eluted fungal proteins from PL-treated C. albicans D7100 are shown in Fig. 1. These results demonstrated a UV dose-dependent increase in both protein leakage and membrane permeability, which was also strongly correlated with a commensurate decrease in cell viability over similar PL treatment regimes. 15.3 ± 0.5 µg/ml of fungal protein was lost from the cell after 150 pulses (or UV dose of 4.1 µJ/cm^2), which corresponded to a 7.8 log order reduction in cell viability (Fig. 1). A similar pattern of protein loss with increased PL exposure was exhibited by all C. albicans strains tested ($r^2 = 0.89$) (data not shown).

Plasma membrane permeabilisation in response to PL was estimated by fluorescence microscopy based on the influx of PI that is excluded by test yeast cells with intact plasma membranes. The proportions of C. albicans test cells exhibiting PI permeability were plotted versus increasing exposure to PL at 7.2 J (Fig. 2). PL-treated cells demonstrated increased PI fluorescence in response to increasing amounts of UV exposure. This UV dose-dependent increase in cell permeability correlated strongly with a commensurate decrease in cell viability in PL treatment (Fig. 2). During the initial 15 pulses of PL-irradiation (UV dose 0.41 µJ/cm^2) less than 1% of treated cell were found to exhibit PI permeability (Fig. 2). However, following 20 pulses (UV dose 0.55 µJ/cm^2) there was an exponential increase in the numbers of PI positive cells with a corresponding decrease in cell viability. After 90 and 150 pulses (equivalent to UV doses of 2.4 and 4.1 µJ/cm^2 respectively), approximately 90% and 99% of treated yeast cells displayed PI fluorescence. The overall trend observed with the PI cellular uptake assay was consistent with that observed with the protein leakage assay for similarly treated samples; suggesting that loss of plasma membrane selective permeability coincides with loss of membrane integrity with increasing exposure to PL-irradiation.

The latter highlights the importance of cell membrane integrity and functionally in maintaining viable clinically-relevant yeast. Previous studies have shown that the ability of yeast to cope with environmental stresses that affect plasma membrane organisation and functionality depends upon maintenance of its physical characteristics such as organization of fatty acyl chains in the phospholipid membrane (van der Rest et al., 1995). A similar phenomenon was observed by Takeshita et al. (2003), who noted that the concentration of eluted proteins varied significantly between pulsed light and low-pressure UV (LP-UV) irradiated yeast cell suspensions, with LP-UV treated samples showing minimal protein leakage. These
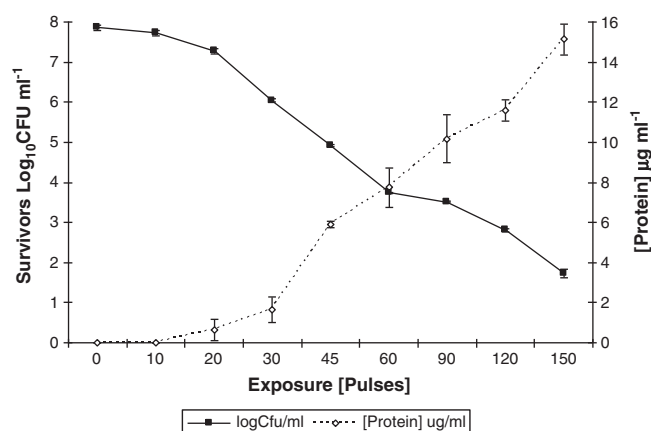

Fig. 1. Reduction in total fungal proteins levels (µg/ml) in C. albicans D7100 as a consequence of increased pulsing or amount of pulses applied.
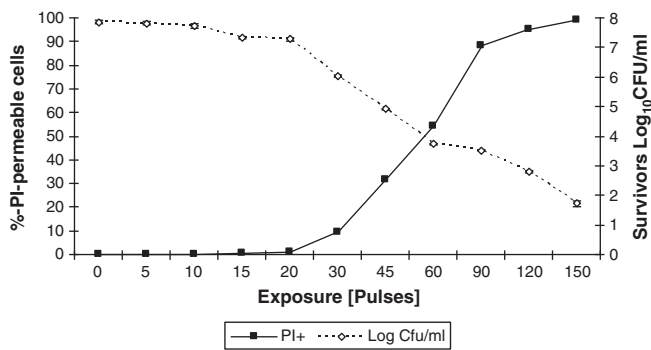
Fig. 2. Relationship between pulsed light inactivation of *C. albicans* D7100 and prodidium iodide (% PI) permeable cells.

authors reported that this observed difference in cell membrane integrity post UV irradiation may be attributed to the contribution of spectral components of pulsed light that is not present in LP-UV lamp spectrum. Other researchers have reported previously that exposing *Saccharomyces cerevisiae* cells to near-UV radiation (300–400 nm) caused damage to the yeast cell membrane functionality due to loss of permeability and to membrane-associated active transport processes (Arami et al., 1993).

3.2. Generation of reactive oxygen species (ROS) in UV irradiated test yeast

Oxidative stress is an unavoidable consequence of life in an oxygen-rich atmosphere. Oxygen radicals and other activated oxygen species are generated as by-products of aerobic metabolism and exposure to various natural and synthetic toxicants. Redox homeostasis in cells is important for the maintenance of proper cellular functions (Adler et al., 1999) including intracellular communication (Karu, 2008) as well as initiation and propagation of apoptosis (Madeo et al., 1999). Elevated levels of intracellular reactive oxygen species (ROS) can be biologically deleterious, potentially damaging a wide range of macromolecules including nucleic acids, proteins and lipids. The production of intracellular ROS was monitored in test yeast during the course of PL-treatments using the specific ROS mitochondrial stain dihydrorhodamine-123 (DHR-123) and cytosolic stain 2′,7′-dichlorodihydrofluorescein diacetate (DCFH-DA). Previous researchers have that DRH is no fluorescent, uncharged, and readily taken up by cells, whereas DHR-123, the product of DHR oxidation, is fluorescent, is positively charged, and binds selectively to the inner mitochondrial membrane of living cells (Royall and Ischiropoulos, 1993; Qin et al., 2008). Qin et al. (2008) reported that the fluorescence of this dye is an indicator of mitochondrial reactive oxygen intermediate production and membrane integrity. Our findings revealed a distinct shift in the localisation of intracellular ROS generation in test yeast over the 150 pulse regime at 7.2 J (Figs. 3, 4 and 5). A low basic level of ROS with distinct mitochondrial localisation was initially observed within the first 20 pulses by visualization of DHR-123 fluorescence, which also included localised ROS clusters about the periphery of the cells (data not shown). A sudden drop in mitochondrial ROS levels was observed after 20 pulses in PL-treated test yeast with a subsequent steady UV dose-dependent increase in ROS levels occurring with increased pulsing. Maximal levels of ROS induced fluorescence were observed following 20 pulses at 7.2 J, with similar levels observed after the terminal 150 pulse end point.

The ROS profile measured using the cytosolic specific 2′,7′-dichlorofluorescein (DCFH-DA) stain revealed a significantly different pattern of activity in similarly treated PL-samples (Fig 4). Previous researchers have reported that DCFH-DA is also readily taken up by cells and, after deacetylation to DCFH, is oxidised to its fluorescent
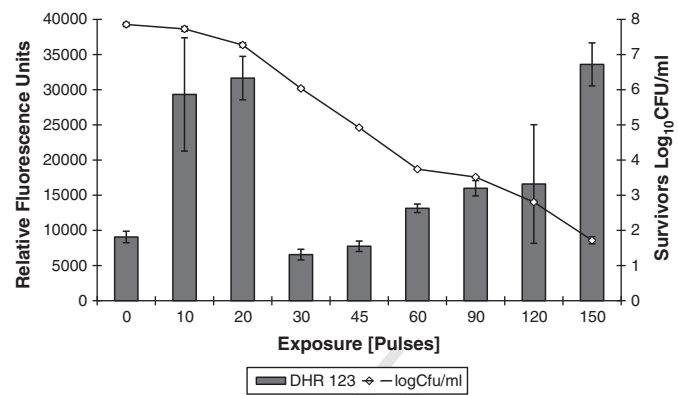

Fig. 3. Relationship between mitochondrial ROS generation and localization profile as measured by specific DHR-123 fluorescence and microbial inactivation (Survivors Log_{10} CFU/ml) in pulsed-light treated *C. albicans* D7100.

derivative, DCF, and remains in the cytosol (Royall and Ischiropoulos, 1993; Qin et al., 2008). The DCFH-DA method has become a standard technique for measuring ROS formed in cells by ionizing radiation (Hafer et al., 2008). The DCFH-DA plot for PL-treated cell suspensions demonstrated marginally increased levels from 30 pulses (corresponding to DHR-123 pattern) with a substantial dose-dependent increase in ROS load evident at 90, 120 and 150 pulse end-points. The levels of cytosolic ROS observed following 150 pulses in test yeast were approximately 20 times those observed following 30 pulses and 10 times those observed following 90 pulses in similarly treated samples at 7.2 J. DCFH can be oxidised by several reactive species, including RO_2, RO, OH, HOCl, and $ONOO^-$, but only longer-lived radicals contribute to the increase in fluorescence (Ischiropoulos et al., 1999).

The intracellular superoxide levels in PL-treated yeast were measured using the ROS stain dihydroethidium (DHE) (Fig. 5). This superoxide-specific stain had been used successfully by other research groups to investigate ROS activity in microbial cultures (Carter et al., 1994; Henderson and Chappell, 1993). The oxidation of DHE to ethidium (ET) is relatively specific for O_2^-, with minimal oxidation induced by H_2O_2, $ONOO^-$, HOCl (Tarpey and Fridovich, 2001). DHE is dehydrogenated to ethidium, which then intercalates with negatively charged DNA and emits a red fluorescent signal. Our findings showed that PL-treated samples demonstrated a UV dose-dependent increase in intracellular superoxide levels (Fig. 5). Specifically, a UV dose-dependent increase in superoxide levels was observed following 30 pulses, which culminated in ca 98% of PL-treated yeast cells exhibiting intense DHE-mediated fluorescence
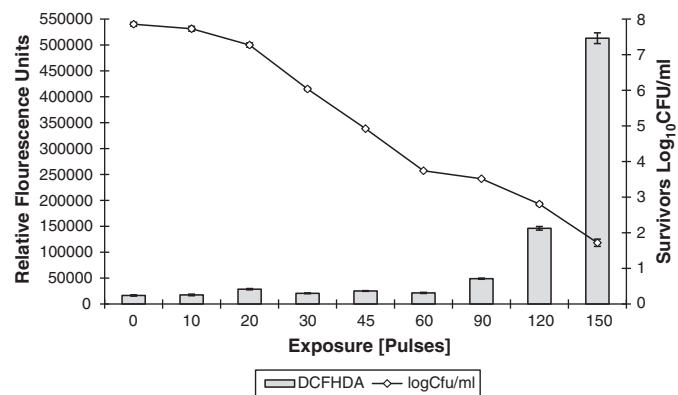

Fig. 4. Relationship between cytosolic ROS generation and localization profile as measured by specific DFCH-FA fluorescence and microbial inactivation (Survivors Log_{10} CFU/ml) in pulsed light treated *C. albicans* D7100.
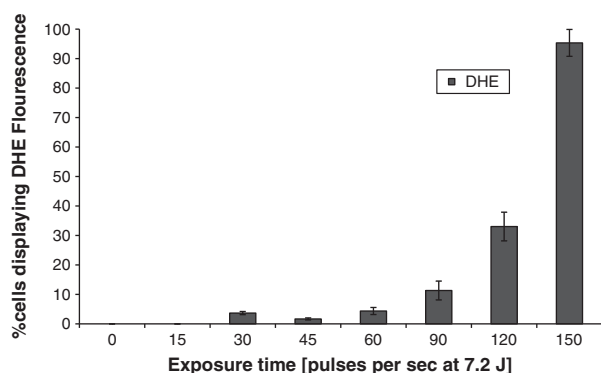
Fig. 5. Percentage of *C. albicans* D7100 exhibiting DHE fluorescence over 150 pulsing regime at lamp discharge energy of 7.2 J.

following 150 pulses (Fig. 5). The presence of high levels of superoxide anion at higher PL exposures is in agreement with the observations of Rowe et al. (2008) who noted that as the redox state of yeast cells continues to move toward an oxidised state as a consequence of high levels of DNA damage caused by increased intracellular levels of O_2^-, such ROS-stressed cell can no longer survive due to extensive nuclear and macromolecular damage. There was a degree of variation observed in ROS levels between the strains, however, the patterns of distribution remained consistent where all strains exhibited enhanced ROS activity when exposed to increased amount of pulsing [data not shown].

Under normal physiological conditions, intracellular ROS generated during respiration are retained by the mitochondria and reduced by protective enzymes such as superoxide dismutase, catalase and glutathione peroxidise (Chang et al., 2004). However, a reduction in protective enzyme activity or an event such as mitochondrial membrane depolarisation can result in the accumulation of ROS in the cytoplasm that imparts an oxidative stress burden on the cell (Gourlay and Ayscough, 2005) The diversity of ROS species that can be generated in cells is matched by a variety and complexity of cellular responses to detoxification, repair of damage, or maintenance of metal ion homeostasis, with at least 450 genes required to maintain cellular resistance to ROS (Perrone et al., 2008). Such intracellular defence mechanisms in yeast involve antioxidant enzymes, such as Q5 superoxide dismutases (SODs), catalases and peroxidises (Kwon et al., 1994) are susceptible to damage by ROS. Previous studies have demonstrated that oxidative processes result in the loss of key antioxidant enzymes (Hodgson and Fridovich, 1975; Kono and Fridovich, 1982; Tabatabaie and Floyd, 1994), which may exacerbate oxidative stress-mediated cytotoxicity (Lee et al., 2001). A reduction in superoxide-dismutase activity has been shown to reduce cell viability (Longo et al., 1996; Wawryn et al., 1999). Both superoxide dismutase and catalase are readily deactivated by singlet oxygen and by the radicals (Escobar et al., 1996). Thus, there is a growing consensus that ROS, such as hydroxyl radicals, superoxide anions, and organic hydroperoxides, play a role in cellular damage caused by ionizing radiation such as DNA strand breaks, lipid peroxidation and protein modification (Lee et al., 2001). Lee et al. (2001) showed that cytosolic and mitochondrial SODs play an essential role in the protection of yeast cells against ionizing radiation. This observation is further supported by the significant increases in ROS levels such as superoxide and organic hydroperoxides in PL-treated *C. albicans* strains in this present study.

3.3. Role of PL-mediated lipid peroxidation of cellular membranes on the viability of treated yeast

Lipid hydroperoxides are prominent non-radical intermediates of lipid peroxidation whose identification can often provide valuable mechanistic information such as whether a primary reaction is mediated by singlet oxygen or oxyradicals (Girotti et al., 1985). The endogenous oxidative degradation of membrane lipids by lipid peroxidation result in the formation of a very complex mixture of lipid hydroperoxides, chain-cleavage products, and polymeric material (Girotti, 1998). Once initiated, lipid peroxidation can self-perpetuate as a radical chain reaction, impairing membrane integrity and membrane-associated functions (Alic et al., 2001; Davis, 2000). The presence of lipid peroxides in PL-treated yeast was determined using the peroxiDetect™ Kit (Fig. 6). Examination of the findings for lipid peroxidation production in this study (Fig. 6) revealed a similar pattern of microbial lethality aligned with enhanced protein leakage (Fig. 1) and PI fluorescence (Fig. 2) due to increased pulsing. Test yeast demonstrated a dramatic initial increase in lipid hydroperoxide levels with c.a. 26, 43 and 67 nM peroxide ml/L measured following 45 (UV dose 1.24 µJ/cm^2), 90 (UV dose 2.48 µJ/cm^2) and 150 (UV dose 4.13 µJ/cm^2) pulses at 7.2 J respectively. This also corroborates previous observations from other research groups which reported that peroxidised membranes become rigid and lose their selective permeability and integrity when exposed to lethal extrinsic stresses (Davis, 2000). Lipid hydroperoxides are by-products of the interaction of ROS with lipid components of plasma membrane. Examination of the results outlined in Fig. 6 revealed a UV dose dependent increase in the levels of lipid hydroperoxides in response to increasing exposure to PL irradiation. There was also a strong correlation between increasing levels of lipid hydroperoxides and decreasing cell viability.

The relationship between intracellular ROS generation, lipid peroxidation and cellular responses to sub-lethal and lethal stress exposures is best understood by examination of the model outlined by Girotti (1998). Under normal physiological growth condition, the cell is in homeostasis with a pro-oxidant/antioxidant balance. However, exposure to low levels of an oxidant inducing stress such as PL causes low levels of lipid peroxidation in treated cell membranes of test yeast. There also appears to be a threshold for repair in PL-treated test yeast that was limited to the first 20 pulses (UV dose 0.55 µJ/cm^2). With moderate levels of lipid peroxidation, stress signalling may lead to the death program induction culminating in apoptotic death. Higher levels of PL-mediated lipid peroxidation in test yeast caused structural and metabolic damage leading to cell membrane lysis (Figs. 1 and 2) and necrotic cell death became evident (Fig. 7). The loss of membrane selective permeability is further supported by the presence of extracellular aqueous hydroperoxides and superoxide anions that accumulate after increasing amounts of high pulsed light exposures [data not shown]. Arami et al. (1997) demonstrated that photo-decomposition of ergosterol following exposure to near-UV radiation caused cell death. This may also be in part attributed to alteration to the sterol structure as a result of singlet oxygen-mediated oxidation of ergosterol in the plasma membrane of PL-
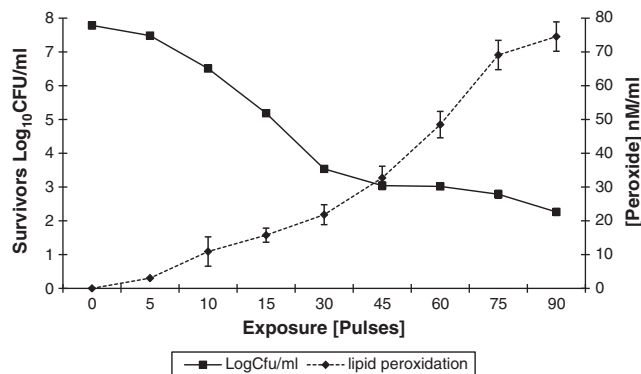

Fig. 6. Relationship between lipid peroxidation (mM/ml) and microbial cell reductions (Survivors Log$_{10}$ CFU/ml) in pulsed UV light treated *C. albicans* D7100.
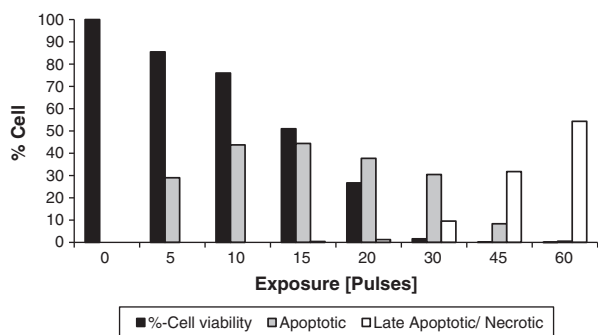
Fig. 7. Percentage occurrence of apoptotic (late and early) and necrotic *C. albicans* D7100 cells at various end-point determinations post pulsed light exposure at 7.2 J.

treated yeast leading to the formation of oxysterols that do not optimally support membrane function and cell growth (Böcking et al., 2000). Such alterations in the structure and functioning of ergosterol in PL-treated yeast may cause destabilisation of membrane with commensurate loss of fluidity leading to cell death. Böcking et al. (2000) also indicated that the fatty acid composition of cellular membrane lipids accounted for different sensitivities to oxidative damage, where the cell membrane also acts as a primary site for oxidative attack. These findings indicate that irreversible disruption of cell membrane functionality contributes to PL mediated inactivation in clinical-relevant *C. albicans*.

3.4. Determination of apoptosis and necrosis in PL-treated C. albicans

Apoptosis is a highly regulated form of programmed cell death in higher eukaryotes. Apoptosis is defined by a set of cytological alterations including externalisation of lipid phosphatidylserine (PS), chromatin condensation, DNA breakage and uncontrolled accumulation of ROS (Madeo et al., 2002). DNA fragmentation and formation of membrane-enclosed cell fragments termed "apoptotic bodies" (Martin et al., 1995) also occurs. Programmed cell death is found in many eukaryotes and is crucial for embryogenesis, tissue homeostasis and disease control in multicellular organisms (Madeo et al., 2002). Recently, it was discovered that simple unicellular organisms like budding *S. cerevisiae*, *Candida* spp., *Aspergillus* and bacteria also have the potential to undergo apoptosis (Phillips and Vousden, 2001; Madeo et al., 2002). Measurement of DAPI-stained yeast cells post PL-treatments in this study (data not shown) revealed fuzzy and prolate spheroid chromatin characteristics typical of apoptotic cell phenotypes. These PL-treated cells showed sickle-shaped DNA (ca. 1–10% of treated cells) and randomly distributed nuclear fragments (ca. 10–40% of treated cells) after 30 pulses (UV dose 0.82 $\mu J/cm^2$). Increased fragmentation was observed with subsequent PL treatments beyond 30 pulses with 80–90% of the cells displaying abnormal chromatin distribution.

The translocation of lipid PS from the inner leaflet to the extracellular side of the plasma membrane is recognised as an early stage event in apoptosis and was detected using Annexin V that has a strong affinity for PS. When combined with PI that stains DNA of injured cells with permeable membranes, this combined Annexin V/PI staining approach facilitates distinction of early apoptotic (designated as Annexin V^+/PI^-), late apoptotic (designated as Annexin V^+/PI^+) and necrotic (designated as Annexin V^-/PI^+) cells. These differences, where apoptotic and necrotic yeast cells emitted green light and red fluorescence respectively, allowed discrimination of apoptotic and late apoptotic/necrotic cells (Fig. 7). Early and late stage apoptosis was confined to the initial 30 to 45 pulses in treated test yeast. Following 5 pulses approximately 30% demonstrated early-stage apoptotic cell characteristics with maximal Annexin V^+/PI^- types evident after 15 pulses. The latter measure of cell injury also coincides with the localisation of mitochondrial ROS in similarly treated cells. After augmented PL-treatments the numbers of early-stage apoptotic cells decreased significantly with only 38, 31 and 4% of cells exhibiting this Annexin V^+/PI^- characteristic after 20, 30 and 45 pulses respectively (Fig. 7). Following 15 pulses a UV dose-dependent increase in the numbers of PI^+ cell types was observed with ca. 10% displaying late apoptotic or Annexin $^+/PI^+$ characteristics. After 45 pulses (UV dose 1.24 μ/cm^2) cells were characterised as being late apoptotic or necrotic in appearance. A marked pattern emerged where with increased pulsing a decrease in late-apoptotic type cells occurred that was matched by an increase in necrotic cell (Annexin$-/PI^+$) numbers, with only necrotic cells observed following 150 pulses at 7.2 J. This general pattern was not unexpected as previous researchers have reported that numerous cytotoxic substances that cause necrosis when applied at elevated concentrations also induce apoptosis in similar cells when used at lower concentrations (Liberthal and Levin, 1996). However, to the best of the author's knowledge no other study exploring the occurrence of apoptosis in PL-treated microorganisms has been published.

Akin to mammalian cells, apoptosis in yeast cells can be induced by cell–cell communication, by external stresses such as conventional UV, toxins, starvation, heat or by reactive oxygen species (Madeo et al., 1999; del Carratore et al., 2002). One of the key factors differentiating apoptotic and necrotic cell death is the utilisation of energy by the former phenotype. Apoptosis is an energy dependent process and, therefore, if the energy depletion occurs above a critical threshold then necrosis will ensue (Gabai et al., 2000). Therefore, the mitochondria are not only important for the energetic status of the cell but are also pivotal organelles governing microbial life and death (Eisenberg et al., 2007). Damage to mitochondrial macromolecules may also lead to increased ROS production and further damage to mitochondrial components thereby causing a vicious downward spiral in terms of ROS production and damage accumulation in yeast cells (Madeo et al., 2002). Perrone et al. (2008) proposed that increased ROS production is due to reduced oxygen consumption by respiratory chain, which is associated with increased availability of intracellular oxygen for ROS production. Interestingly, the presence of extensive intracellular levels of ROS early in PL treatments (Figs. 3, 4 and 5) coincided with the appearance of apoptotic cell phenotypes. Another feature of apoptotic cell death process is an increase in the intracellular levels of superoxide anion (Simon et al., 2002), which also occurred in PL-treated cells as measured by mitochondrial ROS specific DHR-123 staining (Fig. 3). However, it is not clear as to what event comes first, the generation or accumulation of intracellular ROS leading to cell death, or the onset of apoptosis leading to cellular damage resulting in augmented ROS production in treated cells.

As with mammalian cell, yeast has an asymmetric distribution of phospholipids within the cytoplasmic membrane. However, on induction of apoptosis 90% of lipid phosphatidylserine (PS) that are initially orientated towards the cytoplasm are translocated to the outer leaflet (Martin et al., 1995). Therefore, lipid PS exposure serves as a sensitive marker for early stage apoptosis, which was detected in PL-treated *C. albicans* test strains using annexin V stain that has a high binding affinity for PS in the presence of Ca^{2+}. Also, other research groups have recently stated that an apoptotic yeast cell, such as *C. albicans* treated with acetic acid (Phillips and Vousden, 2001), will eventually suffer from a collapse of metabolism causing the breakdown of plasma membrane integrity leading to the appearance of a necrotic morphology. Eisenberg et al. (2010) have recently reported that the process of necrosis may still be regulated by defined molecular events, which is distinguishable from unregulated necrosis inflicted by brutal chemical or physical insults such as by PL-irradiation reported in this study. However as the effects are pleiotropic, further studies are needed in order to establish whether PL-induced apoptosis in *C. albicans* is initiated by general damage responses or by the alteration of specific cellular components.

3.5. Use of comet assay to investigate nuclear damage in PL-irradiated test yeast

The comet assay is a widely adopted rapid and sensitive technique for detecting and analyzing the potential of substances to cause DNA damage which includes strand breaks, alkali-labile sites, DNA cross-links, and incomplete excision repair sites in virtually all singles (Tice et al., 2000; Kirf et al., 2010). The basic principle of the comet assay is the migration of different sized DNA molecules in an agarose gel under an electrophoretic current. More specifically, induced DNA strand breakage leads to fragmentation of the supercoiled duplex DNA which can be stretched out by electrophoresis. Under an electric current, due to their reduced molecular size, fragments of damaged DNA move further within the pores of the agarose gel than intact DNA. This process leads to the microscopic appearance of the cell as a comet-like shape as the broken strands of the negatively changed DNA molecule become free to migrate in the electric field toward the anode. The intact DNA of the nucleus form the head of the comet and the small DNA fragments appear as the tail. The presence of strand breaks in PL-treated test yeast was visualized after 15 pulses (UV dose $0.41\ \mu J/cm^2$) by the emergence of comet tails from the nuclei of the cells (Fig. 8). Greater tail moment and tail DNA were observed with enhanced pulses in treated test yeast ($p < 0.05$). This constitutes the first occasion where the comet assay was used to confirm that damage to DNA occurs in PL-treated test yeast. Examination of test yeast post PL-treatments revealed that *C. albicans* did retain some capacity for repair that occurred within the first 20 pulses (or UV dose $0.55\ \mu J/cm^2$) (Fig. 9). Previous researchers have reported that germicidal effect of PL-irradiation on pathogenic yeast is related in-part to the formation of pyrmidine dimmers inhibiting formation of new DNA that derails the process of cell replications (referred to as clonogenic death) (Farrell et al., 2009). This trend also coincides with the large variation in colony size and appearance that was observed in PL-treated test yeast
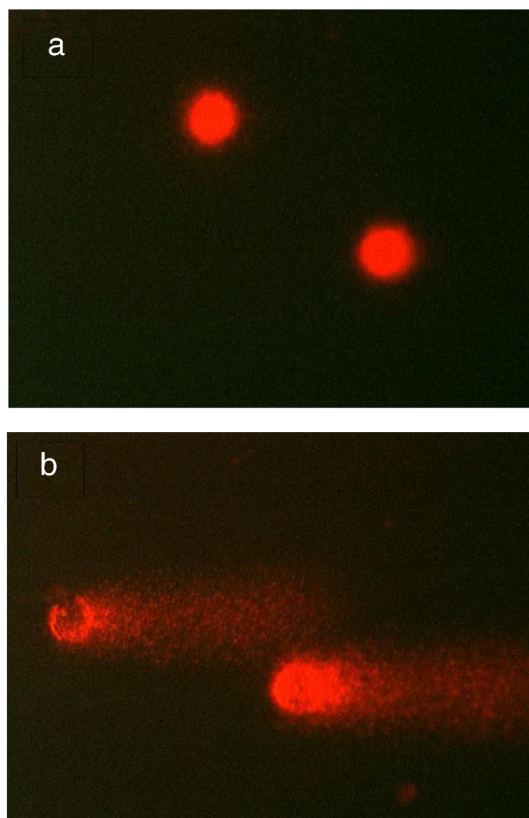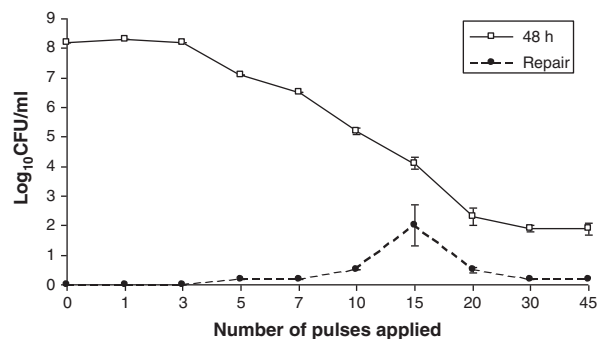
Fig. 9. Examination of the levels of *C. albicans* D7100 repair (expressed in Survivors Log_{10} CFU/ml) after exposure to pulsed light at 7.2 J/pulse.

following 24 and 48 h incubation at 30 °C. This difference in colony size and appearance was absent or less pronounced in similar samples exposed to more lethal levels of PL (60 pulses or UV does $1.65\ \mu J/cm^2$). It is therefore likely that vital pathways mediating repair of damaged DNA in test yeast (such as direct reversal, base excision repair, nucleotide excision repair, mismatch repair, translesion synthesis and recombination direct reversal as reported by Rowe et al., 2008) are either decoupled or unable to function properly in PL-treated cells that also experience simultaneous damage to other vital cellular components. An early response of mitotic cells to low level stress injury is to enter a transient growth-arrested state in which the DNA is largely supercoiled, replication is halted and only a few stress genes are transcribed and translated (Crawford et al., 1996; Davis, 2000). This is not unexpected given the high levels of ROS measured PL treated test yeast in this study. Only when the cell is damaged severely by ROS, resulting in delay in cell division and some apoptosis, are specific antioxidant and repair functions induced strongly (Alic et al., 2004). **Q10** Therefore, it is probable that a proportion of the PL-treated test yeast entered growth arrest as a protective measure against oxidative stress and were able to repair associated damage. If the oxidative stress is not severe enough to cause apoptosis or necrosis, cells will re-enter the growth cycle after a period of transient growth arrest (Davis, 2000). This would account for the appearance of new colonies following 48 h incubation, which were not observed during enumeration following 24 h incubation. Takeshita et al. (2003) reported that greater level of **Q11** DNA damage occurs using conventional low-pressure UV light compared with treating similar *S. cerevisiae* samples with pulsed light.

Despite the fact that PL-irradiation has been approved for food surface decontamination by the US Food and Drug Administration (FDA) since 1999, significant variability in the efficacy of PL for treating similar spoilage and pathogenic microorganisms has been reported (Oms-Oliu et al., 2010). While the main mechanism of **Q12** microbial inactivation is explained through photochemical effect that prevents the treated cell from replicating (Wang et al., 2005), our findings have also demonstrated that photophysical effects also play a significant contributory role in PL-mediated microbial lethality. Krishnamurty et al. (2008) also reported that PL-treated *Staphylococ-* **Q13** *cus aureus* exhibited cell wall damage, cytoplasmic membrane shrinkage, cellular content leakage, and mesosome disintegration based on visualization with transmission electron microscopy and Fourier transform infrared spectroscopy observations.

4. Conclusion

Our findings clearly demonstrated that PL-irradiation inactivates *C. albicans* through a multi-hit cellular process that includes inflicting irreversible damage to DNA and destabilizing the functionality and integrity of plasma cell membranes. These findings have significant implications for PL-technology development, in particular for surface and water decontamination applications. PL has also significant

Fig. 8. Fluorescent images of DNA from untreated (a) and pulsed light-treated (b) *C. albicans* D7100 post comet assay.

potential applications for the treatment of packaging material surfaces or food contact materials that require rapid disinfection, particularly as this approach is characterised by the lack of residual compounds that eliminates the need for use of chemical disinfectants and preservatives (Oms-Oliu et al., 2010). Despite growing evidence to support use of PL for the aforementioned applications, there is a pressing need to identify an intracellular marker such as onset of late apoptosis or early stage necrosis in PL-treated microbial pathogens so as to standardize and optimise treatments for different applications. Our findings clearly demonstrate that onset of necrosis in PL-treated *C. albicans* reflects lethality and can be used as an *in-vitro* real-time marker to confirm disinfection efficacy. Our findings have also significant broader implications as it is envisaged that this approach may be adopted, in time, as a complementary or alternative method to that of using conventional plate count and redox probes for the real-time detection of microbial lethality post decontamination. These conventional viability methods used to confirm disinfection efficacy are limited by the recognised fact that a sub-population of treated microorganisms may be capable of repair after resuscitation (Rowan, 2011). Whereas, confirmation of the detection of a late necrotic marker in PL-treated microorganisms appears to be related to a treatment regime that inflicts irreversible damage and is beyond that identified by use of plate count and possibly vital respiratory or redox staining. Our findings also corroborate the viewpoint of Guerrero-Beltrán and Barbosa-Cánovas (2004), which highlights the need to optimise all inter-related factors to achieve target inactivation level for specific food applications.

Q14

Additional future studies should focus on investigating and confirming that the relationship between microbial lethality and onset of necrosis in a broad range of PL-treated microbial spoilage and pathogenic microorganisms is an accurate and repeatable measurement of PL-process efficiency. Additional studies also merited including use of more ROS specific probes such as *N*-can-acetyl-3, 7-dihydroxyphenoxazine (Amplex Red) and 2-[6-(4′-hydroxy) phenoxy-3 H-xanthen-3-on-9-yl] benzoic acid (HPF) for the determination of OH$^{.}$ and H_2O_2 levels respectively, which will help unravel roles of specific reactive oxygen species in PL-mediated cell death process. There is also the possibility that visible light component of the PL lamp spectrum contributed to yeast inactivation, which was not specifically investigated in this study. It is known that endogenous protoporphyrin IX is an efficient photosensitiser of photodynamic processes in biological objects exposed to visible light (Shumarina et al., 2003). The phototoxicity of endogenous protoporphyrin IX is due to its ability to generate ROS (predominantly singlet oxygen), which readily react with biologically important macromolecules and thereby cause their photo-oxidation, impairment of their functional activity and eventually cell death.

Q15
5. Uncited references

Apel and Hirt, 2004
Blank and Shoenfield, 2004
Fröhlich and Madeo, 2000
Gardner and Fridovich, 1991
Gralla and Kosman, 1992
Ludovico et al., 2002
Marquenie et al., 2003

References

Adler, V., Yin, Z., Tew, K.D., Ronai, Z., 1999. Role of redox potential and reactive oxygen species in stress signaling. Oncogene 18, 6104–6111.

Alic, N., Higgins, V.J., Dawes, I.W., 2001. Identification of a *Saccharomyces cerevisiae* gene that is required for G_1 arrest in response to the lipid oxidation product linoleic acid hydroperoxide. Mol. Biol. Cell 12, 1801–1810.

Apel, K., Hirt, H., 2004. Reactive oxygen species: metabolism, oxidative stress, and signal transduction. Ann. Rev. Plant Biol. 55, 373–399.

Arami, S., Hada, M., Itadani, A., Yamashita, S., Hachiya, K., Kanayama, M., Tada, M., 1993. Damage of the membrane function in the yeast *Saccharomyces cerevisiae* by near-UV irradiation. Scientific Reports of the Faculty Agriculture Okayama University, 82, pp. 1–7.

Arami, S., Ada, M., Tada, M., 1997. Reduction of ATPase activity accompanied by photodecomposition of ergosterol by near-UV irradiation in plasma membranes prepared from Saccharomyces cerevisiae. Microbiology 143, 2465–2471.

Blank, M., Shoenfield, Y., 2004. Antiphosphatidylserine antibodies and reproductive failure. Lupus 13, 661–665.

Böcking, T., Barrow, K.D., Netting, A.G., Chicott, T.C., Coster, H.G., Hofer, M., 2000. Effects of single oxygen on membrane sterols in the yeast *Saccharomyces cerevisiae*. Eur. J. Biochem. 267, 1607–1618.

Carter, W.O., Narayanan, P.K., Robinson, J.P., 1994. Intracellular hydrogen peroxide and superoxide anion detection in endothelial cells. J. Leukocyte Biol. 55, 253–256.

Chang, T.-S., Cho, C.-S., Park, S., Yu, S., Kang, S.W., Rhee, S.G., 2004. Peroxiredoxin III, a mitochondrion-specific peroxidase, regulates apoptotic signaling by mitochondria. J. Biol. Chem. 279, 41975–41984.

Crawford, D.R., Schools, G.P., Salmon, S.L., Davies, K.J.A., 1996. Hydrogen peroxide induces the expression of *adapt15*, a novel RNA associated with polysomes in hamster HA-1 cells. Arch. Biochem. Biophys. 325, 256–264.

Davis, K.J.A., 2000. Oxidative stress, antioxidant defenses, and damage removal, repair, and replacement systems. IUBMB Life 50, 279–289.

de Repentigny, L., Daniel Lewandowski, D., Jolicoeur, P., 2004. Immunopathogenesis of oropharyngeal candidiasis in human immunodeficiency virus infection. Clin. Microbiol. Rev. 17, 729–759.

del Carratore, R., Della Croce, C., Simili, M., Taccinie, E., Scavuzzo, M., Sbrana, S., 2002. Cell cycle and morphological alterations as indicative of apoptosis promoted by UV irradiation in *S. cerevisiae*. Mutation Res 513, 183–191.

Eisenberg, T., Bultner, S., Kroemer, G., Madeo, F., 2007. The mitochondrial pathways in yeast apoptosis. Apoptosis 12, 1011–1023.

Eisenberg, T., Carmona-Gutierrez, D., Büttner, S., Tavernarakis, N., Madeo, F., 2010. Necrosis in yeast. Apoptosis 15, 257–268.

Elmnasser, N., Guillou, S., Leroi, F., Orange, N., Bakhrouf, A., Federighi, M., 2007. Pulsed-light system as a novel food decontamination technology: a review. Can. J. Microbiol. 53, 813–821.

Escobar, J.A., Rubio, M.A., Lissi, E.A., 1996. SOD and catalase inactivation by singlet oxygen and peroxyl radicals. Free Radical Med. 20, 285–290.

Fanello, S., Bouchara, J.-P., Jousset, N., Delbos, V., LeFlohic, A.-M., 2001. Nosocomial *Candida albicans* acquisition in a geriatric unit: epidemiology and evidence for person-to-person transmission. J. Hosp. Infect. 47, 46–52.

Farrell, H.P., Garvey, M., Rowan, N.J., 2009. Studies on the inactivation of medically important *Candida* species on agar surfaces using pulsed light. FEMS Yeast Res. 9, 956–966.

Farrell, H.P., Garvey, M., Cormican, M., Laffey, J.G., Rowan, N.J., 2010. Investigation of critical inter-related factors affecting the efficacy of pulsed light for inactivating clinically relevant bacterial pathogens. J. Appl. Microbiol. 108, 1494–1508.

Fröhlich, K.-U., Madeo, F., 2000. Apoptosis in yeast—a monocellular organism exhibits altruistic behaviour. FEBS Lett. 473, 6–9.

Gabai, U.L., Vaglom, J.A., Volloch, U., Merlin, A.B., Force, T., Koutroumanis, M., Massie, B., Mosser, D.D., Sherman, M.Y., 2000. Hsp72-mediated suppression of c-jun n-terminal kinase is implicated in development of tolerance to caspase independent cell death. Mol. Cell. Biol. 20, 6828–6836.

Gardner, P.R., Fridovich, I., 1991. Superoxide sensitivity of the *Escherichia coli* aconitase. J. Biol. Chem. 266, 19328–19333.

Garvey, M., Farrell, H.P., Cormican, M., Rowan, N.J., 2010a. Investigations of the relationship between use of *in vitro* cell culture-quantitative PCR and a mouse-based bioassay for evaluating critical factors affecting the disinfection performance of pulsed light for treating *Cryptosporidium parvum* oocysts in saline. J. Microbiol. Methods 80, 267–273.

Garvey, M., Farrell, H.P., Cormican, M., Rowan, N.J., 2010b. Investigations of the relationship between use of *in vitro* cell culture-quantitative PCR and a mouse-based bioassay for evaluating critical factors affecting the disinfection performance of pulsed light for treating *Cryptosporidium parvum* oocysts in saline. J. Microbiol. Methods 80, 267–273.

Girotti, A.W., 1998. Lipid hydroperoxide generation, turnover and effector action in biological systems. J. Lipid Res. 39, 1529–1542.

Girotti, A.W., Thomas, J.P., Jordan, J.E., 1985. Inhibitory effect of zinc (II) on free radical lipid peroxidation in the erythrocyte membranes. J. Free Radical Biol. Med. 1, 385–401.

Gómez-López, V.M., Ragaert, P., Debevere, J., Devlieghere, F., 2007. Pulsed light for food decontamination: a review. Trends Food Sci. Technol. 18, 464–473.

Gourlay, C.W., Ayscough, K.R., 2005. The actin cytoskeleton: a key regulator of apoptosis and ageing? Nature Rev. Mol. Cell Biol. 6, 583–589.

Gralla, E.B., Kosman, D.J., 1992. Molecular genetics of superoxide dismutases in yeasts and related fungi. Adv. Genetics. 30, 251–319.

Guerrero-Beltrán, J.A., Barbosa-Cánovas, G.V., 2004. Review: advantages and limitations on processing foods by UV light. Food Sci. Technol. Intern. 10, 137–147.

937 Hafer, K., Konishi, T., Schiestl, R.H., 2008. Radiation-induced long lived extracellular
938   radicals do not contributed to measurement of intracellular reactive oxygen species
Q16   using dichlorofluorescein method. Radiat. Res. 169 489–473.
940 Helmerhorst, E.J., Breeuwer, P., van 't Hof, W., Walgreen-Weterings, E., Oomen, L.C.J.M.,
941   Veerman, E.C.I., Nieuw Amerongen, A.V., Abee, T., 1999. The cellular target of
942   histatin 5 on Candida albicans is the energized mitochondrion. J. Biol. Chem. 274,
943   7286–7291.
944 Henderson, L.M., Chappell, J.B., 1993. Dihydrorhodamine 123: a fluorescent probe for
945   superoxide generation? Eur. J. Biochem. 217, 973–980.
946 Herker, E., Jungwirth, H., Lehmann, K.A., Maldener, C., Fröhlich, K.U., Wissing, S.,
947   Büttner, S., Fehr, M., Sigrist, S., Madeo, F., 2004a. Chronological aging leads to
948   apoptosis in yeast. J. Cell Biol. 164, 501–507.
949 Herker, E., Jungwirth, H., Lehmann, K.A., Maldener, C., Fröhlich, K.-U., Wissing, S.,
950   Büttner, S., Fehr, M., Sigrist, S., Madeo, F., 2004b. Chronological aging leads to
951   apoptosis in yeast. J. Cell Biol. 164, 501–507.
952 Hodgson, E.K., Fridovich, I., 1975. The interaction of bovine erythrocyte superoxide
953   dismutase with hydrogen peroxide: inactivation of the enzyme. Biochemistry 14,
954   5294–5299.
955 Hsu, M.C., Chen, K.W., Lo, H.J., Chen, Y.C., Liao, M.H., Lin, Y.H., Li, S.Y., 2003. Species
956   identification of medically important fungi by use of real-time LightCycler PCR. J.
957   Med. Microbiol. 23, 1071–1076.
958 Ischiropoulos, H., Gow, A., Thom, S.R., Kooy, N., Royall, J.A., Crow, J.P., 1999. Detection of
959   reactive nitrogen species using 2, 7-dichlorodihydrofluorescein and dihydrorho-
960   damine 123. Methods Enzymol. 301, 367–373.
961 Jiang, Z., Woollard, A.C.S., Wolff, S.P., 1991. Lipid peroxide measurement by oxidation of
962   Fe^{++} in the presence of xylenol orange: comparison with the thiobarbituric acid
963   assay and an iodometric method. Lipids 26, 853–856.
964 Karu, T.I., 2008. Mitochondrial signaling in mammalian cells activated by red and near-
965   IR radiation. Photochem. Photobiol. 84, 1091–1099.
966 Kirf, D., Higginbotham, D.L., Rowan, N.J., Devery, S.M., 2010. Cyto- and genotoxicological
967   assessment and functional characterization of N-vinyl-2-pyrrolidone–acrylic acid-
968   based copolymeric hydrogels with potential for future use in wound healing
969   applications. Biomed. Mater. 5.
970 Klassen, R., Meinhardt, F., 2004. Induction of DNA damage and apoptosis in
971   Saccharomyces cerevisiae by a yeast killer toxin. Cell. Microbiol. 7, 393–401.
972 Kono, Y., Fridovich, I., 1982. Superoxide radical inhibits catalase. J. Biol. Chem. 257,
973   5751–5754.
974 Krishnamurty, K., Tewari, J.C., Irudayaray, J., Demirici, A., 2008. Microscopic and
975   spectroscopic evaluation of inactivation of Staphylococcus aureus by pulsed UV light
976   and infrared heating. Food Bioproc. Technol. doi:10.1007/s11947-008-0084-8
977 Lee, J.H., Choi, I.Y., Kil, I.S., Kim, S.Y., Yang, E.S., Park, J.W., 2001. Protective role of
978   superoxide dismutases against ionizing radiation in yeast. Biochim. Biophys. Acta
979   1526, 191–198.
980 Liberthal, W., Levin, J.S., 1996. Mechanisms of apoptosis and its potential role in renal
981   tubular epithelial cell injury. Am. J. Physiol. 271, 477–488.
982 Longo, V.D., Gralla, E.B., Valentine, J.S., 1996. Superoxide dismutase activity is essential
983   for stationary phase survival in Saccharomyces cerevisiae: mitochondrial production
984   of toxic oxygen species in vivo. J. Biol. Chem. 27, 12275–12280.
985 Ludovico, P., Rodrigues, F., Almeida, A., Silva, M.T., Barrientos, A., Côrte-Real, M., 2002.
986   Cytochrome c release and mitochondria involvement in programmed cell death
987   induced by acetic acid in Saccharomyces cerevisiae. Mol. Biol. Cell 13, 2598–2606.
988 Madeo, F., Fröhlich, E., Ligr, M., Grey, M., Sigrist, S.J., Wolf, D.H., Fröhlich, K.U., 1999.
989   Oxygen stress: a regulator of apoptosis in yeast. J. Cell Biol. 145, 757–767 K.U..
990 Madeo, F., Englhardt, S., Herker, E., Lehmann, X.I., Maldener, C., Proksch, A., Wissing, S.,
991   Fröhlich, K.U., 2002. Apoptosis in yeast: a new system with applications in cell
992   biology and medicine. Curr. Gen. 41, 208–216.
993 Marquenie, D., Michiels, C.W., Van-Impe, J.F., Schrevens, E., Nicolai, B.N., 2003. Pulsed
994   white light in combination with UV-C and heat to reduce storage rot of strawberry.
995   Postharvest Biol. Technol. 28, 455–461.
996 Martin, S.J., Reutelingsperger, C.P., McGahon, A.J., Rader, J.A., van Schie, R.C., LaFace, D.
997   M., Green, D.R., 1995. Early redistribution of plasma membrane phosphatidylserine
998   is a general feature of apoptosis regardless of the initiating stimulus: inhibition by
999   overexpression of Bcl-2 and Abl. J. Exper. Med. 182, 1545–1556.
1061

1000 Miloshev, G., Mihaylov, I., Anachkova, B., 2002. Application of the single cell gel
1001   electrophoresis on yeast cells. Mutation Res. 513, 69–74.
1002 Nomura, K., Imai, H., Koumura, T., Arai, M., Nakagawa, Y., 1999. Mitochondrial
1003   phospholipid hydroperoxide glutathione peroxidase suppresses apoptosis medi-
1004   ated by a mitochondrial death pathway. J. Biol. Chem. 274, 29294–29302.
1005 Nugent, M.J.D., Higginbotham, C.L., 2007. Preparation of a novel freeze thawed poly
1006   (vinly alcohol) composite hydrogel for drug delivery applications. Eur. J. Pharma.
1007   Biopharm. 67, 377–386.
1008 Oms-Oliu, G., Martin-Belloso, O., Soliva-Fortuny, R., 2010. Pulsed light treatments for
1009   food preservation. A review. Food Bioproc. Technol. 3, 13–23.
1010 Perrone, G.G., Tan, S.X., Dawes, I.W., 2008. Reactive oxygen species and yeast apoptosis.
1011   Bioch. Biophys. Acta. Mol. Cell. Res. 1783, 1354–1368.
1012 Phillips, A.C., Vousden, K.H., 2001. E2F-1 induced apoptosis. Apoptosis 6, 173–182.
1013 Qin, Y., Lu, M., Gong, X., 2008. Dihydrorhodamine 123 is superior to 2, 7-
1014   dichlorodihydrofluorescein diacetate and dihydrorhodamine 6 G in detecting
1015   intracellular hydrogen peroxide in tumor cells. Cell Biol. Intern. 32, 224–228.
1016 Rahn, R.O., Stefan, M.I., Bolton, J.R., Goren, E., Shaw, P.S., Lykke, K.R., 2003. Quantum
1017   yield of the iodide–iodate chemical actinometer: dependence on wavelength and
1018   concentration. Photochem. Photobiol. 78, 146–152.
1019 Rowan, N.J., 2011. Defining established and emerging microbial risks in the aquatic
1020   environment: current knowledge, implications and outlooks. Inter. J. Microbiol.
1021   doi:10.1155/2011/462832
1022 Rowan, N.J., MacGregor, S.J., Anderson, J.G., Fouracre, R.A., McIlvaney, L., Farish, O., 1999.
1023   Pulsed-light inactivation of food-related micro-organisms. Appl. Environ. Micro-
1024   biol. 65, 1312–1315.
1025 Rowe, L.A., Degtyareva, N., Doetsch, P.W., 2008. DNA damage-induced reactive oxygen
1026   species (ROS) stress response in Saccharomyces cerevisiae. J. Free Radical Biol. Med.
1027   45, 1167–1177.
1028 Royall, J.A., Ischiropoulos, H., 1993. Evaluation of 2′, 7′-dichlorofluorescein and
1029   dihydrorhodamine 123 as fluorescent probes for intracellular H2O2 in cultured
1030   endothelial cells. Arch. Biochem. Biophys. 302, 348.
1031 Shumarina, A.O., Strakhovskaya, M.G., Turovetskii, V.B., Fraikin, G.Y., 2003. Photody-
1032   namic damage to yeast subcellular organelles induced by elevated levels of
1033   endogenous protoporphyrin IX. Microbiology 72, 434–437.
1034 Simon, H.U., Hay-Yehia, A., Levi-Schaffer, F., 2002. Role of reactive oxygen species in
1035   apoptosis induction. Apoptosis 5, 415–418.
1036 Solberg, C.O., 2000. Spread of Staphylococcus aureus in hospitals: causes and prevention.
1037   Scand. J. Infect. Dis. 32, 587–595.
1038 Tabatabaie, T., Floyd, R.A., 1994. Susceptibility of glutathione peroxidase and
1039   glutathione reductase to oxidative damage and the protective effect of spin
1040   trapping agents. Arch. Biochem. Biophys. 314, 112–119.
1041 Takeshita, K., Shitato, J., Sameshima, T., Fukunaga, S., Isobe, S., Arihara, K., Itoh, M., 2003.
1042   Damage of yeast cells induced by pulsed light irradiation. Intern. J. Food Microbiol.
1043   85, 151–158.
1044 Tarpey, M.M., Fridovich, I., 2001. Methods of detection of vascular reactive species.
1045   Nitric oxide, superoxide, hydrogen peroxide, and peroxynitrite. Circ. Res. 89,
1046   224–236.
1047 Tice, R.R., Agurell, E., Anderson, D., Burlinson, B., Hartmann, A., Kobayashi, H., Miyamal,
1048   Y., Rojas, E., Ryu, J.-C., Gasaki, Y.F., 2000. Single cell gel/comet assay: guidelines for
1049   in vitro and in vivo genetic toxicology testing. Environ. Mol. Mutagenesis 35,
1050   206–221.
1051 van der Rest, M.E., Kamminga, A.H., Nakano, A., Anraku, Y., Poolman, B., Konings, W.N.,
1052   1995. The plasma membrane of Saccharomyces cerevisiae: structure, function and
1053   biogenesis. Microbiol. Rev. 59, 304–322.
1054 Virto, R., Mañas, P., Álvarez, I., Condon, S., Raso, J., 2005. Membrane damage and
1055   microbial inactivation by chlorine in the absence and presence of a chlorine-
1056   demanding substrate. Appl. Environ. Microbiol. 71, 5022–5028.
1057 Wang, T., MacGregor, S.J., Anderson, J.G., Woolsey, G.A., 2005. Pulsed ultra-violet
1058   inactivation spectrum of Escherichia coli. Water Res. 39, 2921–2925.
1059 Wawryn, J., Krzepilko, A., Myszka, A., Bilinski, T., 1999. Deficiency in superoxide
1060   dismutases shortens life span of yeast cells. Acta Biochim. Pol. 46, 249–353.